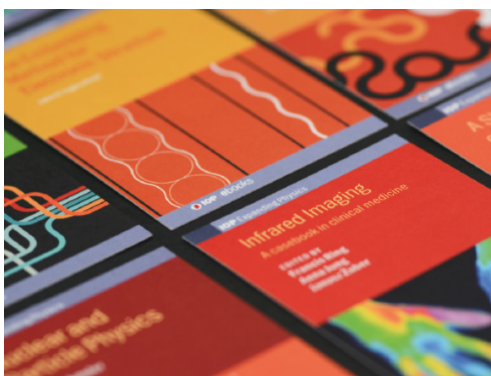# Raman and infrared spectra of KNbO$_3$ in niobate glass-ceramics

To cite this article: J S de Andrade *et al* 1999 *J. Phys.: Condens. Matter* **11** 4451

View the article online for updates and enhancements.

Raman and infrared spectra of KNbO$_3$ in niobate glass–ceramics

J S de Andrade†‡, A G Pinheiro‡, I F Vasconcelos‡, J M Sasaki‡,
J A C de Paiva‡, M A Valente§ and A S B Sombra‡

† Centro de Tecnologia, Universidade de Fortaleza-UNIFOR, Brazil
‡ Laboratório de Óptica não Linear e Ciência dos Materiais (LONLCM), Departamento de Fisica,
Universidade Federal do Ceará, Caixa Postal 6030, CEP 60455-760 Fortaleza-Ceará, Brazil
§ Departamento de Fisica, Universidade de Aveiro, Campus Universitário de Santiago,
3810 Aveiro, Portugal

E-mail: sombra@ufc.br

Abstract. Potassium niobophosphate glasses and glass–ceramics of the family $[x\text{Nb}_2\text{O}_5.(50-x)$ $\text{P}_2\text{O}_5.50\text{K}_2\text{O}]:y\text{Fe}_2\text{O}_3$ were studied by x-ray powder diffraction, infrared and Raman scattering spectroscopy. For the potassium–phosphate samples [50P$_2$O$_5$–50K$_2$O] the iron oxide presents a network former behaviour, for 2 mol% of Fe$_2$O$_3$ doping. The precipitation of crystalline K$_4$Nb$_6$O$_{17}$ and ferroelectric KNbO$_3$ crystals was confirmed by x-ray powder diffraction in the samples with $x = 40$ and 50 mol% respectively. The infrared and Raman scattering spectroscopy results suggest that the increase of the ratio Nb$_2$O$_5$/P$_2$O$_5$ leads the niobium to sites of octahedral symmetry and consequently to the formation of ferroelectric KNbO$_3$, as seen by x-ray diffraction analysis.

1. Introduction

Optical glasses containing Nb$_2$O$_5$ are of great interest because of their application as nonlinear photonic materials [1, 2], and as laser hosts having high stimulated emission parameters [3]. However, unlike silicate and phosphate-based glasses, very little research has been done on niobate-based glasses. The role played by Nb$_2$O$_5$ in the glass structure, the coordination state of Nb^{5+} and the interaction with other elements in the glass network is still a subject under study. Rachkovskaya and Bubkova [4] have studied glasses of P$_2$O$_5$–Nb$_2$O$_5$– V$_2$O$_5$–TiO$_2$ and P$_2$O$_5$–Nb$_2$O$_5$–TiO$_2$–Fe$_2$O$_3$ by infrared spectroscopy. They have found evidence of the existence of NbO$_4$ and NbO$_6$ units. Fukumi and Sakka [5], using Raman spectroscopy, confirmed that there are NbO$_6$ polyhedra in the glass network of K$_2$O–Nb$_2$O$_5$–SiO$_2$. The effect of iron doping and associated vacancies in P$_2$O$_5$–PbO–Nb$_2$O$_5$–K$_2$O–Fe$_2$O$_3$ glasses has been studied by thermally stimulated depolarization currents and Mössbauer spectroscopy [6].

There has been an increasing academic and technologic interest in glasses containing ferroelectric crystals as nonlinear optical materials [7]. Potassium niobate (KNbO$_3$) is among those oxide materials that respond to light-induced space charges by large changes in the refractive index. The crystals thus are well suited for photorefractive applications [8]. It is also a very interesting material for the study of the ferroelectric phase transitions, because it undergoes a cubic–tetragonal–orthorhombic–rhombohedral phase change sequence [9]. Moreover, in contrast to other perovskite compounds such as BaTiO$_3$ and PbTiO$_3$, single domain samples can be available, in practice, in the four phases. The room temperature othorhombic phase

was specially investigated by neutron scattering [10], Raman scattering [11] and infrared reflectivity experiments. For this and other reasons $KNbO_3$ has been extensively used for optical applications.

In this paper we describe the fabrication of a series of potassium niobophosphate-based glasses, $[xNb_2O_5.(50 - x)P_2O_5.50K_2O]:yFe_2O_3$, with $0 \leqslant x \leqslant 50$ mol% and $y = 2$ mol%, and their characterization by x-ray diffraction, infrared and Raman scattering spectroscopies. The main goal of the present work is to understand the formation processes of niobophosphate glass and glass ceramics. Ferroelectric $KNbO_3$ was identified by the x-ray powder diffraction, Raman and IR spectra which is in agreement with data from the literature. The potassium niobate crystals $K_4Nb_6O_{17}$ were identified by the x-ray diffraction, infrared and Raman spectra for $x = 40$ and $x = 50$ mol%. The crystalline phase of KPO_3 was detected in sample A ($x = 0$, $y = 0$ mol%). Such glasses and glass–ceramics containing microcrystallites of ferroelectric materials formed in a controlled crystallization process would be interesting candidates for new optical nonlinear glasses or glass–ceramics.

2. Experimental procedure

Samples were prepared from reagent grade ammonium phosphate ($NH_4H_2PO_4$), lithium carbonate (K_2CO_3), niobium oxide (Nb_2O_5) and with iron oxide Fe_2O_3, by mixing reagents in appropriate proportions and heating them in platinum exposed to air crucibles in an electric furnace. The iron oxide Fe_2O_3 was included as an impurity. To prevent excessive boiling and consequent loss of mass, the water and ammonia in $NH_4H_2PO_4$ were removed by pre-heating the mixture at 200 °C for several hours before the fusion. The mixture was subsequently melted at 1150 °C for 1 hour. The melt was then poured into a stainless steel mould and pressed between two stainless steel plates that yielded samples around 3 mm thick. The stainless steel plates did not receive any special polishing procedure. Batches to give ~10 g of each sample were prepared from the starting materials. The mould and plates were pre-heated to 300 °C. The final glass compositions are $[xNb_2O_5.(50 - x)P_2O_5.50K_2O]:yFe_2O_3$, with $0 \leqslant x \leqslant 50$ mol% and $y = 2$ mol%. For details see table 1.

Table 1. Glass and glass–ceramic systems $[xNb_2O_5.(50 - x)P_2O_5.50K_2O]:yFe_2O_3$, with $0 \leqslant x \leqslant 50$ mol% and $y = 2$ mol%.

Sample	K_2O	P_2O_5	Nb_2O_5	Fe_2O_3
A	50	50		
B	50	50		2
C	50	40	10	2
D	50	30	20	2
E	50	20	30	2
F	50	10	40	2
G	50		50	2

Losses of K_2O and P_2O_5, which are the more volatile, due to our experimental procedure, were around 1 mol% and 0.5 mol%, respectively, as measured by chemical gravimetric methods. A comparable loss has also been reported for lithium phosphate glasses [12], where loss of Li_2O is around 1 to 5 mol%. Because of the low loss detected in our sample preparation, the results are discussed in terms of the nominal starting compositions of the samples (table 1).

The X-ray diffraction (XRD) patterns were obtained at room temperature (300 K) by step scanning using powdered samples. We used five seconds for each step of counting time, with a Cu Kα tube at 40 kV and 25 mA using the geometry of Bragg and Brentano.
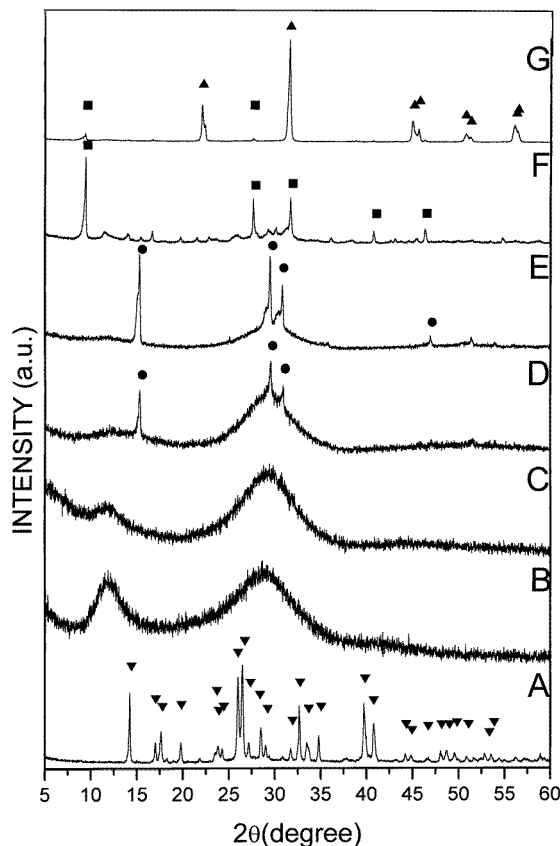
Figure 1. The x-ray powder diffraction pattern of samples A, B, C, D, E, F and G (see table 1). ▲—KNbO$_3$; ■—K$_4$Nb$_6$O$_{17}$; ●—unidentified phase; ▼— KPO$_3$.

The infrared spectra (IR) were measured using KBr pellets made from a mixture of powder for each glass composition. The pellet thickness varied from 0.5 to 0.6 mm. The IR spectra were measured from 1400 to 400 cm^{-1} with a Nicolet 5ZPX FT-IR spectrometer.

The glass transition temperature (T_g), temperature of onset of crystallization (T_x) and the crystallization peak (T_p) were determined by DTA, at heating rate of 10 °C min^{-1} using STA-409 Netzsch apparatus. The DTA measurements were performed using a platinum crucible in air and a constant sample weight of 40 mg was used for all measurements.

Raman spectra were measured with a laser Raman spectrometer using 5145 Å exciting light of the argon laser. The Raman scattering was measured in a back-scattering geometry directly from the powder.

3. Results and discussion

According to the x-ray powder diffraction (XRD) pattern (figure 1), sample A (50K$_2$O–50P$_2$O$_5$) is a ceramic where the KPO$_3$ crystalline phase is easily identified. This is an expected result, according to the literature [13]. For the binary alkali phosphate system, the maximum percentage allowed of the modifier (K$_2$O) is 47 mol% to obtain a glass sample. For our binary glass one has 50 mol% of K$_2$O resulting in a crystallization of the sample.
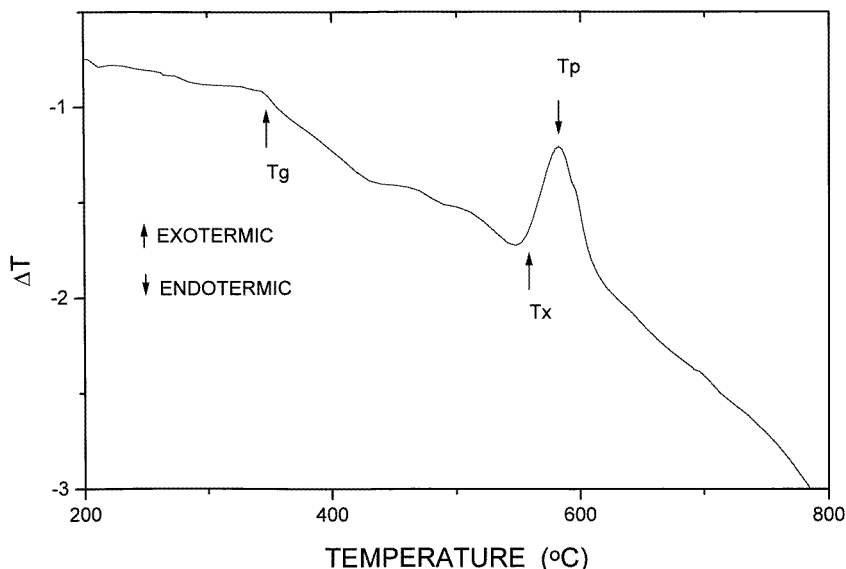
Figure 2. DTA curve of sample B (glass $50K_2O$–$50P_2O_5$:$2Fe_2O_3$).

However with the addition of 2 mol% of Fe_2O_3 we are again in the glass formation region. In figure 1 (curve B) one has the same sample A with the addition of Fe_2O_3. This curve is very characteristic of an amorphous material. This is a very interesting result that is also confirmed by the DTA analysis (figure 2) of sample B. Sample B ($50K_2O$–$50P_2O_5$:$2Fe_2O_3$), a basic composition of the glass family being studied, exhibits an amorphous phase. Figure 2 shows a typical DTA curve of sample B. The glass transition temperature (T_g), temperature of onset of crystallization (T_x) and the crystallization peak (T_p) were determined by DTA. From this curve it is clear that $T_g = 348\,^\circ C$, $T_x = 556\,^\circ C$ and $T_p = 582\,^\circ C$. The difference between T_g and T_x, $T_x - T_g = 200\,^\circ C$, indicates a reasonable stability in these glasses. We believe that the iron oxide is working as a network former in this situation.

Mössbauer spectroscopy studies carried out in lithium niobophosphate glasses [14] shows that in Nb_2O_5 containing glasses, the iron ions essentially occupy octahedra sites working as network modifiers. This observation is in agreement with other Mössbauer results reported in the literature [6]. However in sample B we believe that the iron oxide could have a network former characteristic. However this behaviour will be confirmed with the use of the Mössbauer spectroscopy, in these samples, that is already going on in our laboratories.

Samples with x ranging between zero and 10 mol% (figure 1, samples B and C) only exhibit an amorphous phase, whereas samples with $x = 20$ and 30 mol% exhibit an additional crystalline phase (glass–ceramics) besides the amorphous phase (samples D and E) (see figure 1). The crystalline phase present in these glass–ceramics has not been identified up to this point in our study (figure 1, curves D and E). We believe in the presence of niobium phosphate structures in these phases. If we keep increasing the ratio Nb_2O_5/P_2O_5, the ceramic characteristic of the samples is increasing. In sample F ($x = 40$ mol%) the phase $K_4Nb_6O_{17}$ was identified. In sample G ($x = 50\%$) the potassium niobate, $KNbO_3$, was obtained with a small amount of $K_4Nb_6O_{17}$ which is still present.

Figure 3 shows the IR spectra of samples A, B and C. The absorption spectrum of sample A could be directly associated with the spectrum of the potassium metaphosphate (KPO_3 which
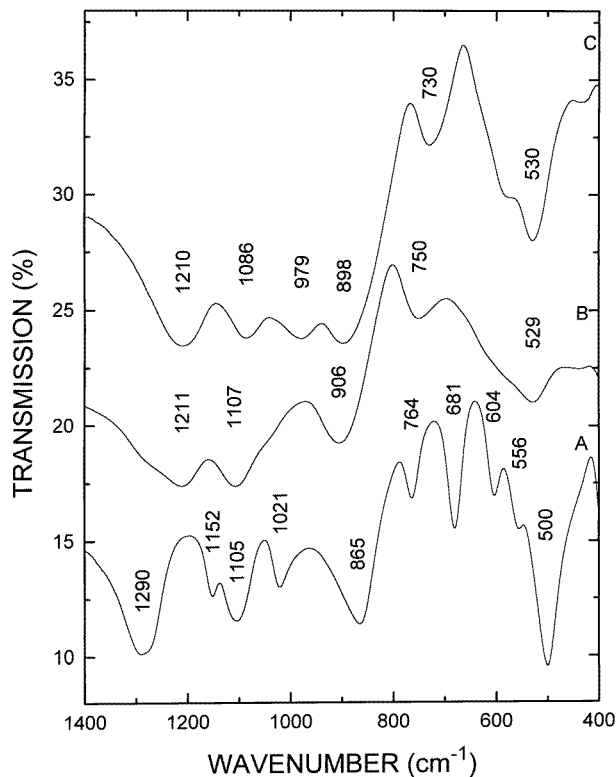
Figure 3. Infrared spectra of the glasses A, B and C (see table 1).

is available in the literature [15]. A dramatic change is observed with the addition of 2 mol% Fe_2O_3 for sample B. The infrared spectrum of sample B is characteristic of a phosphate glass. Assignment of the IR spectral features to phosphate-based glasses has been reported previously [16–18].

According to Muller [17], the absorption of the P=O group is around 1282–1205 cm^{-1} in polymeric phosphate chains. The stretching bands of P–O$^-$ (NBO, non-bridging oxygen) are around 1150/1050 and 950/925 cm^{-1}. Absorptions at 800/720 cm^{-1} are due to P–O–P vibrations (BO, bridging oxygen). The bands below 600 cm^{-1} are due to the bending mode of the PO_4 units phosphate glasses.

Figure 3 (curve B) represents the IR spectrum of the basic potassium phosphate glass. Bands at 1211 cm^{-1} (P=O), 1107 cm^{-1} and 906 cm^{-1} (P–O$^-$) and 750 cm^{-1} and 529 cm^{-1} (P–O–P) are observed. However, the substitution of P_2O_5 by Nb_2O_5 (spectrum C in figure 3) induces changes in the IR spectra. In figure 4 (curve D) the resonances associated with the bridging oxygen (P–O–P) around 730 cm^{-1} and 530 cm^{-1}, for sample C, disappear and a new resonance appears around 600 cm^{-1} (spectra D and E, figure 4). The absence of an infrared absorption band near 1210 cm^{-1} in the samples D and E indicates the absence of the double bonded P=O. The resonances associated with the non-bridging oxygen (P–O$^-$) also decrease with the presence of the Nb_2O_5. This suggests that the niobium oxygen octahedra are using the NBO associated with phosphorous to form the glass network structure.

This observation is also supported by IR data [19], where NbO_6 octahedra exhibit absorption bands around 700 and 610/620 cm^{-1}. In our samples a broad band around 600 cm^{-1} is clearly observed in spectra F and G of figure 4.
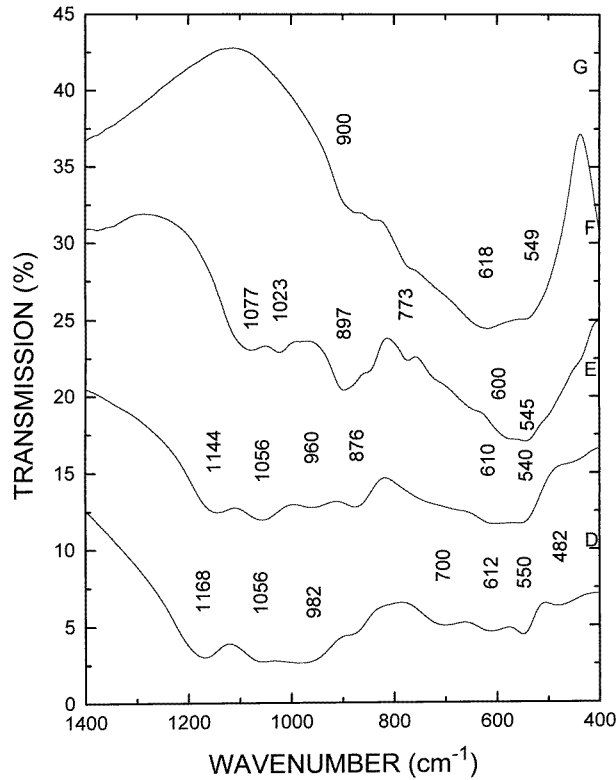
Figure 4. Infrared spectra of the glass ceramics D, E, F and G (see table 1).

Figure 4 shows the infrared spectra of the samples E, F and G, corresponding to glass–ceramics and ceramics whose common characteristic is the presence of a crystalline phase. Note that the IR spectra are strongly modified by this property. In spectrum F, where we have the presence of P_2O_5 and Nb_2O_5, there are major absorptions around 1077 cm^{-1}, 1023 cm^{-1}, 897 cm^{-1} and 773 cm^{-1}, which are probably associated with differently arranged phosphorus–oxygen complexes in the material, and a broad band around 600–545 cm^{-1}. These former bands disappear in spectrum G where the phosphorus is no longer present. The last one is probably associated with the formation of NbO_6 octahedra. The absorptions around 1023 cm^{-1} and 1077 cm^{-1} are associated with the ν_3 antisymmetric stretching vibration of the PO_4 tetrahedra. Reported studies in Li_3PO_4 crystals show that ν_3 are associated with two absorption bands of unequal intensity around 1093 cm^{-1} and 1038 cm^{-1} and ν_4 is related to the absorption around 600 cm^{-1} [20]. This doubling of ν_3 may result from some deformation of the PO_4 tetrahedra, or from vibrational coupling between anions in the same unit cell, or both. The detection of these absorption bands in the IR spectra of our glass–ceramic samples indicates the presence of crystalline phases composed of structures with [PO_4] units. Note that in the spectrum G of figure 4, where we do not have P_2O_5, the absorptions associated with the PO_4 tetrahedra are not observed. The absorption bands around 549 cm^{-1} and 618 cm^{-1} in spectrum G are in good agreement with reported IR spectra of niobate glass–ceramics [19]. These reported results show that the NbO_6 octahedra exhibit two major absorption bands at 700 and $610/620$ cm^{-1}. These bands have been assigned to the ν_3 mode in the corner-shared NbO_6 octahedron [19, 20]. All these assignments are supported by x-ray diffraction results.
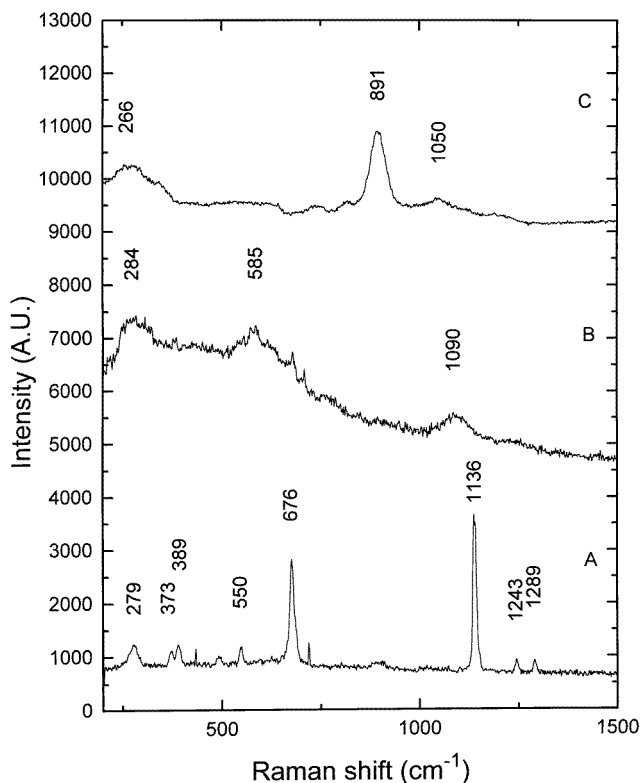
Figure 5. Raman spectra of the samples A, B and C (see table 1).

Figure 1 shows the x-ray powder diffraction of the samples E, F and G. The crystallization of the niobate phase $K_4Nb_6O_{17}$ is quite clear in sample F and decreases with increasing crystallization of $KNbO_3$ as shown in figure 4 (curve G). If the niobium concentration is increased to $x = 50$ mol%, the $KNbO_3$ crystalline phase increases. In figure 1 (curve G), the potassium niobate is easily identified.

To complete the vibrational mode information obtained with IR spectroscopy, we carried out room temperature Raman scattering measurements. These results are represented in figures 5 and 6, respectively. In spectrum A of figure 5 one has the typical Raman spectra of the KPO_3 crystalline phase. The two main peaks, $1136\,cm^{-1}$ and $676\,cm^{-1}$, may be attributed to PO_4 groups. The chain type KPO_3 crystal exhibits the peak at $1136\,cm^{-1}$ which is assigned to the $\nu_s(PO_2)$ mode [21]. The peak observed at $676\,cm^{-1}$ has been assigned to the symmetric P–O–P stretching vibration (ν(P–O–P)sym) of the symmetric PO_2 units, while the modes below $389\,cm^{-1}$ are assigned to the O–P–O bending vibrational mode (ν(O–P–O)).

The 2 mol% of Fe_2O_3 impurity concentration, present in all samples with the exception of sample A, made a strong modification from sample A. Sample B presents strong modifications in the Raman spectra, compared with sample A. The bands present a strong broadening effect which is characteristic of the glass structure.

The spectrum B of figure 5 shows three major bands centred at $284\,cm^{-1}$, $585\,cm^{-1}$ and $1090\,cm^{-1}$. The bands at $1090\,cm^{-1}$ ($\nu_s(PO_2)$ mode), $585\,cm^{-1}$ (ν_s(POP) mode) and the band at $284\,cm^{-1}$ are assigned to bending and torsional vibrations. The spectrum C of figure 5, measured in the sample with 10 mol% of Nb_2O_5, shows three distinct peaks at $266\,cm^{-1}$,
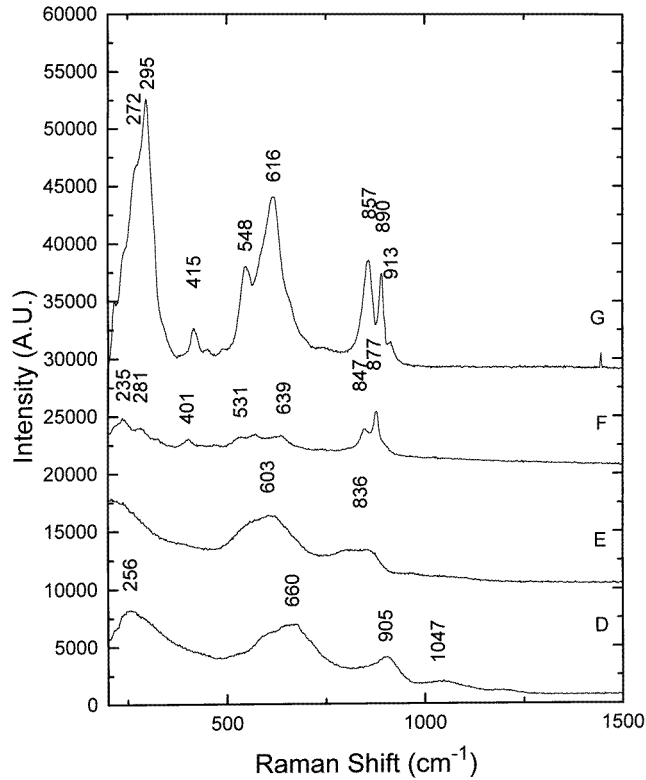
Figure 6. Raman spectra of glass ceramics D, E, F and G (see table 1).

891 cm^{-1} and 1050 cm^{-1}. The 266 cm^{-1} peak is probably associated with vibration modes involving bending and torsional vibrations of the phosphate network, which is also present in sample B. The 891 cm^{-1} peak has been previously assigned to a vibrational mode of Nb–O in octahedral NbO$_6$ or Nb–O–P [22]. Raman scattering studies of gallate glasses show peaks in the Raman shift range between 800 cm^{-1} and 900 cm^{-1}, and between 600 cm^{-1} and 800 cm^{-1}. The former Raman shift range has been attributed to a highly distorted NbO$_6$ octahedra with non-bridging oxygen and the latter to a less distorted NbO$_6$ octahedron with no non-bridging oxygen [5, 23]. The 1050 cm^{-1} peak should be associated with the phosphate group (which is assigned to the $\nu_s(PO_2)$ mode).

In figure 6 (curve D) one has bands around 256 cm^{-1}, 660 cm^{-1}, 905 cm^{-1} and 1047 cm^{-1}. The bands at 256 cm^{-1} (vibration modes involving bending and torsional vibrations), 1047 cm^{-1} ($\nu_s(PO_2)$ mode) are associated with the phosphate structure. The modes 660 cm^{-1} and 905 cm^{-1} are associated with the less and highly distorted NbO$_6$ octahedron with non-bridging oxygen. For sample D the first band is more intense than the second, which is an inverse of the behaviour observed in sample C. In figure 6 (curve E) where we increase the ratio Nb$_2$O$_5$/P$_2$O$_5$ one can observe that the 1047 cm^{-1} band ($\nu_s(PO_2)$ mode), which is present in sample D, almost disappears. In samples D and E one has a glass–ceramic, where the crystalline phase has not yet been identified (see figure 1). In figure 6 (curve F) one has the Raman spectrum of the ceramic K$_4$Nb$_6$O$_{17}$. The spectrum F show a superposition of the modes from crystalline K$_4$Nb$_6$O$_{17}$ with vibrational modes from PO$_4$. The band that goes from 235 to 281 cm^{-1} is associated with PO$_4$ groups present in large part of the ceramic

(vibration modes involving bending and torsional vibrations). The band around 531–639 cm^{-1} in potassium niobophosphate glasses can be attributed to NbO$_6$ octahedra as in silicate glasses [23]. The broad band with peaks at 847 and 877 cm^{-1} is attributed to the NbO$_6$ octahedra with non-bridging oxygens with strong distortion.

In figure 6 (curve G) one has the Raman spectra of the KNbO$_3$ ceramics. The peaks present are all associated with KNbO$_3$ in crystalline form [11]. The first band which is centred at 295 cm^{-1} is probably associated with the A$_1(\nu_{LO})$ mode which in the monocrystal is at 296 cm^{-1}. The peak at 415 cm^{-1} is also associated with the same phonon configuration A$_1(\nu_{LO})$ which in the crystal is at 417 cm^{-1} [11]. The other modes of the A$_1$(LO) phonons are present in the peaks at 548 and 857 cm^{-1}. The A$_1$(TO) phonons are present in the peak at 616 cm^{-1}. The peak observed at 890 cm^{-1} is probably associated with the K$_4$Nb$_6$O$_{17}$ which is still present in sample G according to the x-ray diffraction (see figure 1).

4. Conclusion

Potassium niobophosphate glasses and glass–ceramics of the family $[xNb_2O_5.(50 - x)P_2O_5.50K_2O]:yFe_2O_3$ were studied by x-ray powder diffraction, infrared and Raman scattering spectroscopy. For the potassium–phosphate samples [50P$_2$O$_5$–50K$_2$O] the iron oxide presents a network former behaviour, for 2 mol% of Fe$_2$O$_3$ doping. The precipitation of crystalline K$_4$Nb$_6$O$_{17}$ and the ferroelectric KNbO$_3$ crystals was confirmed by x-ray powder diffraction in the samples with $x = 40$ and 50 mol% respectively. The infrared and Raman scattering spectroscopy results suggest that the increase of the ratio Nb$_2$O$_5$/P$_2$O$_5$ leads the niobium to sites of octahedral symmetry and consequently to the formation of ferroelectric KNbO$_3$, as seen by x-ray diffraction analysis.

References

[1] Vogel E M 1989 *J. Am. Ceram. Soc.* **72** 719
     Vogel E M, Kosinski S G, Krol D M, Jacket J L, Friberg S R, Oliver M and Powers J D 1989 *J. Non-Cryst. Solids* **107** 244
[2] Sombra A S B 1993 *Solid State Commun.* **88** 305
     Sombra A S B 1990 *Opt. Quantum Electron.* **22** 335
     Sombra A S B 1994 *Braz. J. Phys.* **24** 480
[3] Samuneva B, Kvalchev St. and Dimitrov V 1991 *J. Non-Cryst. Solids* **129** 54
[4] Rachkovskaya G E and Bubkova N M 1987 *J. Non-Cryst. Solids* **90** 617
[5] Fukumi K and Sakka S 1988 *J. Mater. Sci.* **23** 2819
[6] de Oliveira C J, de Paiva J A C, Barbosa P C, Mendes Filho J, de Oliveira J C P, Bezerra Sombra A, Aranha N, Barbosa L C and Alves O L 1993 *J. Mater. Sci.* **28** 4305
[7] Komatsu T, Tawarayama H, Mohri H and Matusita K 1991 *J. Non-Cryst. Solids* **135** 105
[8] P Gunter and J P Huignard (eds) 1988 *Photorefractive Materials and their Applications* (Berlin: Springer)
[9] Hewat R 1973 *J. Phys. C: Solid State Phys.* **6** 2559
[10] Currat C, Comes R, Dorner B and Wiesendanger E 1974 *J. Phys. C: Solid State Phys.* **7** 2521
[11] Bozinis D G and Hurrell J P 1976 *Phys. Ver.* B **13** 3109
[12] Abouelleil M M and Leonberger F J 1989 *J. Am. Ceram. Soc.* **72** 1311
[13] Varshneya A K 1994 *Fundamentals of Inorganic Glasses* (New York: Academic) p 118

[14] de Araújo E B, de Paiva J A C, de Araújo M A B and Sombra A S B 1996 *Phys. Status Solidi* **197** 231
     Magalhaes de Abreu J A, de Paiva J A C, Figueiredo R S, de Araújo M A B and Sombra A S B 1997 *Phys. Status Solidi* a **162** 515
     de Almeida E F, de Paiva J A C, de Araújo M A B, de Araújo E B, Eiras J A and Sombra A S B 1998 *J. Phys.: Condens. Matter* **10** 7511
[15] Nyquist R A and Kagel R O 1971 *Infrared Spectra of Inorganic Compounds* (New York: Academic) p 154
[16] Corbridge D E and Lowe E J 1954 *J. Chem. Soc.* I **493**
[17] Muller K P 1969 *Glastech. Ber.* **42** 83
[18] Mogus Milankovic A and Day D E 1993 *J. Non-Cryst. Solids* **162** 275
[19] Tatsumisago M, Hamada A, Minami T and Tanaka M 1983 *J. Non- Cryst. Solids* **56** 423
[20] Tarte P 1967 *J. Inorg. Nucl. Chem.* **29** 915
[21] Nelson C and Tallant D R 1984 *Phys. Chem. Glasses* **25** 31
[22] El Jazouli A, Brochu R, Viala J C, Olazcuaga R, Delmas C and Le Flem G 1982 *Ann. Chim. Fr.* **7** 285
[23] Fukumi K, Kokubo T, Kamiya K and Sakka S 1986 *J. Non-Cryst. Solids* **84** 100